Spectral Difference Solution of Unsteady Compressible Micropolar Equations on Moving and Deforming Grids

Chunlei Liang [1]

[1] Assistant Professor, George Washington University

Applied and Computational Mathematics Division seminar series at NIST in Gaithersburg, MD on Oct. 18th, 2011

1. Motivation
2. Why spectral difference method?
   - Element-wise polynomial reconstruction
   - High-order accuracy even with curved boundary
3. Mathematical Formulation
4. Transform Navier-Stokes and Micropolar equations
5. Elements of the SD method
6. Verification
7. Flow past an oscillating cylinder
8. Flow around a heaving and pitching airfoil past an oscillating cylinder
9. Concluding remark

Sea turtle swimming

Four flippers

Front flippers for thrust generation. Back flipper for steering.

Oscillating wing wind- and hydro- power generator

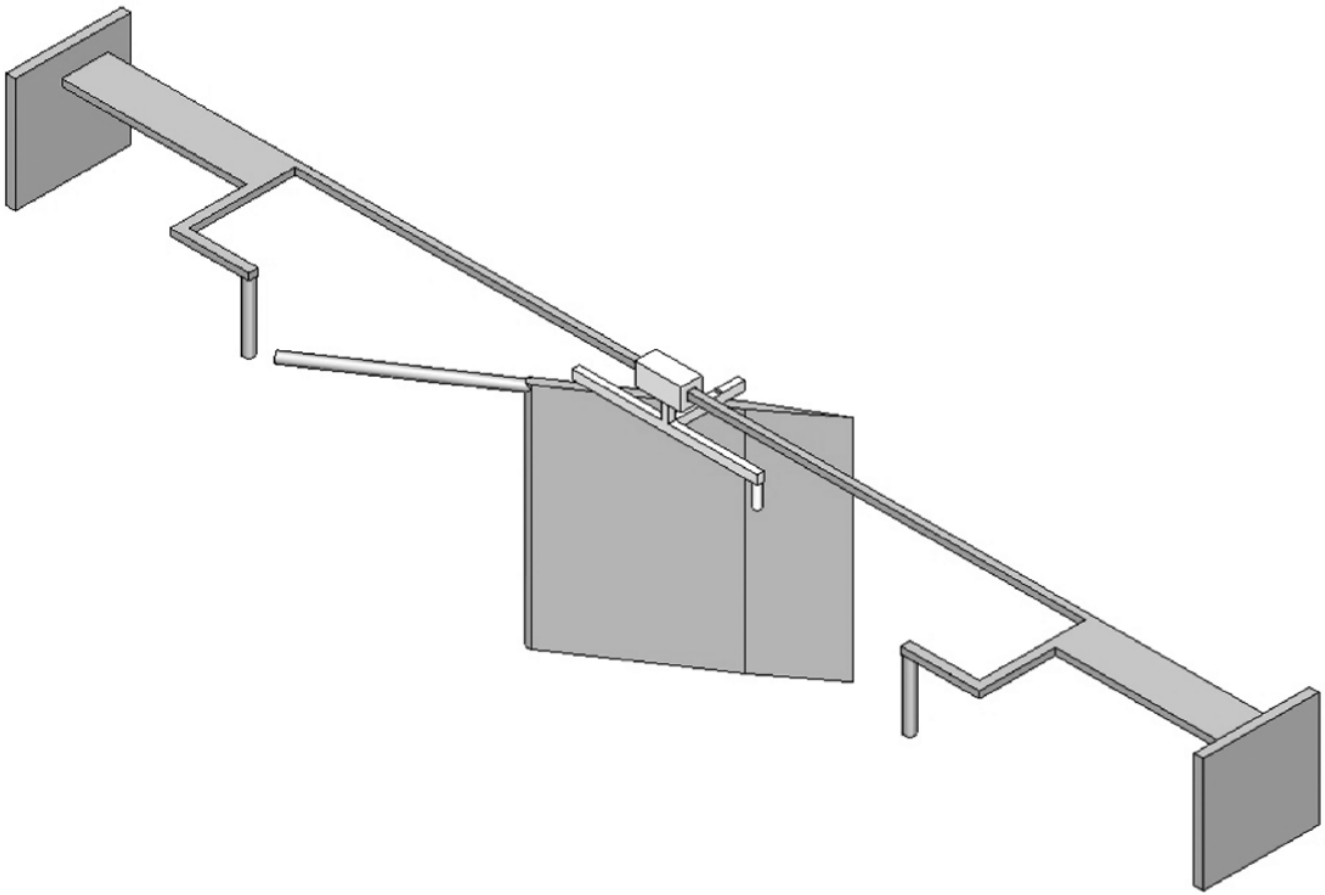

Hydrodynamically controlled wing

Aerohydro Research and Technology Associates.

Plunge-Pitch airfoil for lift generation

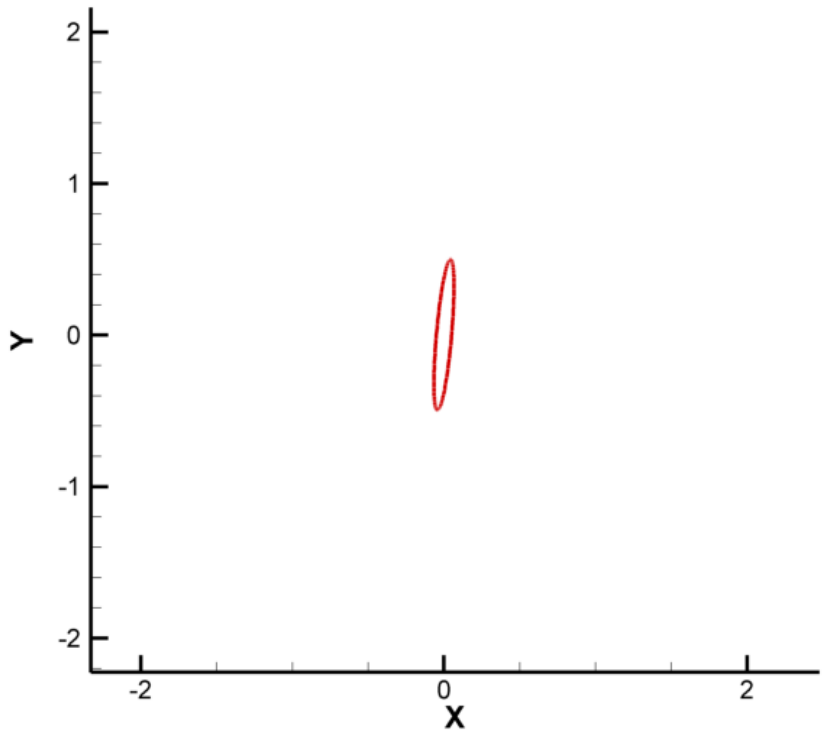

p-refinement

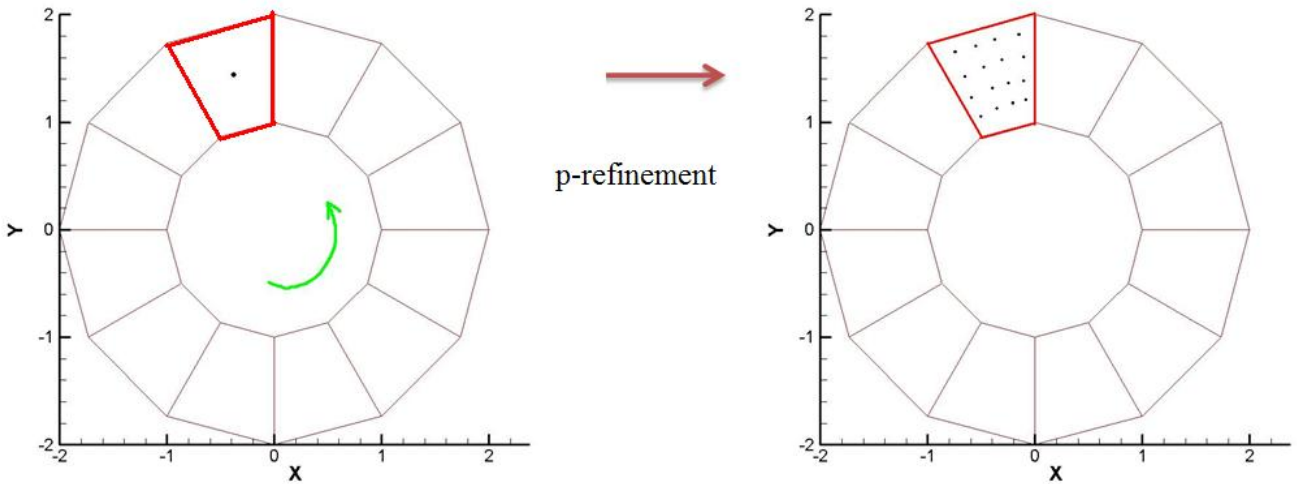

- No re-meshing

p-refinement

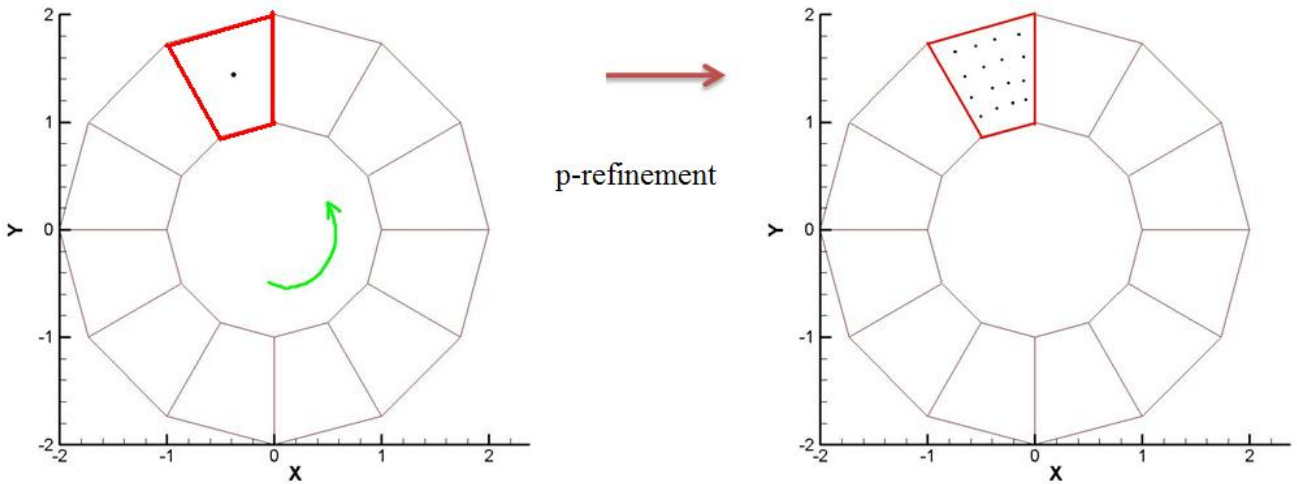

- No re-meshing
- Poor boundary representation

element mapping with high-order curved boundary

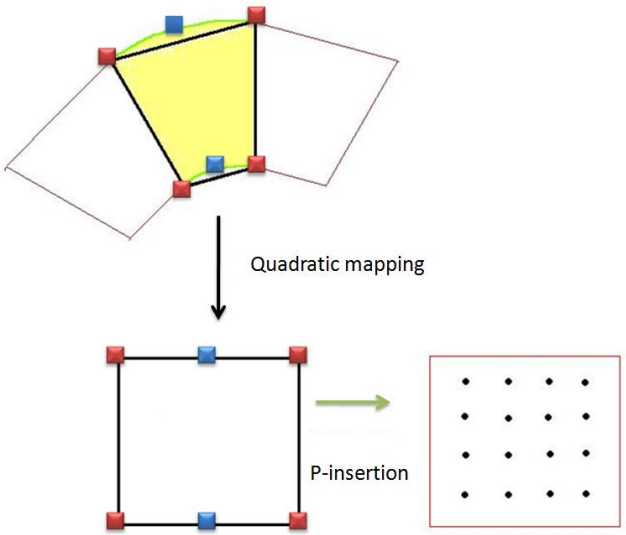

$$\mathcal{J} = \frac{\partial(x,y,t)}{\partial(\xi,\eta,\tau)} = \begin{bmatrix} x_\xi & x_\eta & x_\tau \\ y_\xi & y_\eta & y_\tau \\ 0 & 0 & 1 \end{bmatrix} \quad (1)$$

Key

Universal reconstruction

High-order scheme is attractive for vortex dominated flow

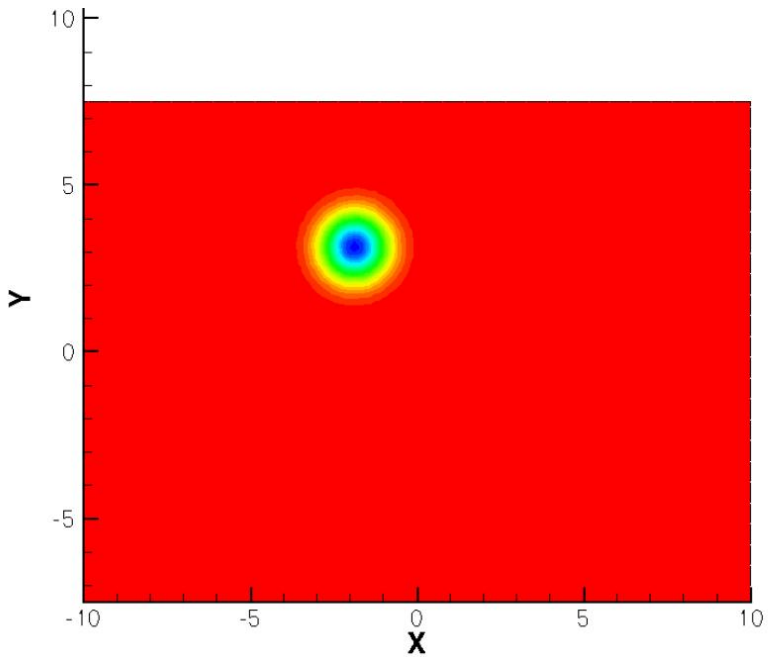

2nd order SD

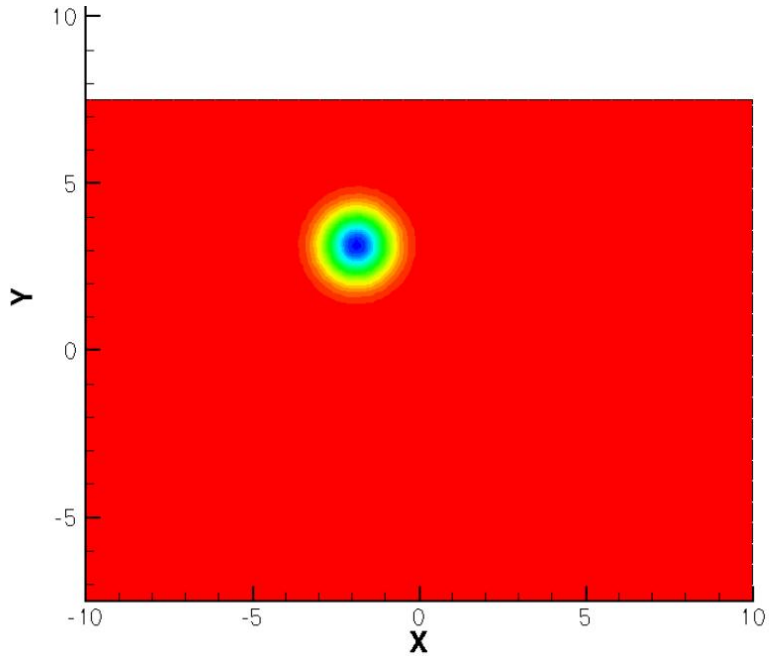

4th order SD

Compressible Navier-Stokes equations

$$\frac{\partial \mathbf{Q}}{\partial t} + \nabla \mathbf{F}_{inv}(\mathbf{Q}) - \nabla \mathbf{F}_{v}(\mathbf{Q}, \nabla \mathbf{Q}) = 0 \tag{2}$$

$$\mathbf{Q} = \left\{ \begin{array}{c} \rho \\ \rho u \\ \rho v \\ E \end{array} \right\}, \quad f_i = \left\{ \begin{array}{c} \rho u \\ \rho u^2 + p \\ \rho uv \\ u(E+p) \end{array} \right\}, \quad g_i = \left\{ \begin{array}{c} \rho v \\ \rho uv \\ \rho v^2 + p \\ v(E+p) \end{array} \right\} \tag{3}$$

$$\frac{f_v}{\mu} = \left\{ \begin{array}{c} 0 \\ 2u_x + \lambda(u_x + v_y) \\ v_x + u_y \\ uf_{v[2]} + vf_{v[3]} + \frac{C_p}{P_r} T_x \end{array} \right\}, \frac{g_v}{\mu} = \left\{ \begin{array}{c} 0 \\ v_x + u_y \\ 2v_y + \lambda(u_x + v_y) \\ ug_{v[2]} + vg_{v[3]} + \frac{C_p}{P_r} T_y \end{array} \right\}$$

Linear constitutive relation

$$t_{ij} = (-p + \lambda a_{mm})\delta_{ij} + (\mu + \kappa)a_{ij} + \mu a_{ji} \tag{4}$$

For Navier-Stokes equations, $a_{ij} = v_{j,i}$;

Micropolar formulation has two deformation tensors

- $a_{ij} = v_{j,i} + e_{jik}\omega_k$;
- $b_{ij} = \omega_{i,j}$.

The same linear relation for heat flux in both N-S and Micropolar formulations, i.e. Fourier's Law:

$$\sigma = \frac{\nu}{Pr} \cdot gradT. \tag{5}$$

Pressure-Energy Relation:

$E = \frac{p}{\gamma - 1} + \frac{1}{2}\rho(u^2 + v^2)$ for Navier-Stokes formulation;

$E = \frac{p}{\gamma - 1} + \frac{1}{2}\rho(u^2 + v^2) + \frac{1}{2}\rho j\omega^2$ for Micropolar formulation.

Micropolar formulation

$$\frac{\partial \mathbf{Q}}{\partial t} + \nabla \mathbf{F}_{inv}(\mathbf{Q}) - \nabla \mathbf{F}_{v}(\mathbf{Q}, \nabla \mathbf{Q}) = \mathbf{S} \tag{6}$$

$$\mathbf{Q} = \begin{Bmatrix} \rho \\ \rho u \\ \rho v \\ \rho j\omega \\ E \end{Bmatrix}, \quad f_i = \begin{Bmatrix} \rho u \\ \rho u^2 + p \\ \rho uv \\ \rho j\omega u \\ u(E+p) \end{Bmatrix}, \quad g_i = \begin{Bmatrix} \rho v \\ \rho uv \\ \rho v^2 + p \\ \rho j\omega v \\ v(E+p) \end{Bmatrix} \tag{7}$$

$$\mathbf{S} = \begin{Bmatrix} 0 \\ 0 \\ 0 \\ \kappa\left(\frac{\partial v_y}{\partial x} - \frac{\partial v_x}{\partial y} - 2\omega\right) \\ 0 \end{Bmatrix} \tag{8}$$

Viscous fluxes of Micropolar equations

$$f_v = \begin{Bmatrix} 0 \\ (2\mu+\kappa)u_x + \lambda(u_x+v_y) \\ \mu(v_x+u_y) + \kappa(v_x-\omega) \\ \Gamma\omega_x \\ uf_{v[2]} + vf_{v[3]} + \omega f_{v[4]} + \frac{\mu C_p}{P_r}T_x \end{Bmatrix} \tag{9}$$

$$g_v(\mathbf{Q}, \nabla\mathbf{Q}) = \begin{Bmatrix} \mu(v_x+u_y) + \kappa(u_y+\omega) \\ (2\mu+\kappa)v_y + \lambda(u_x+v_y) \\ \Gamma\omega_y \\ ug_{v[2]} + vg_{v[3]} + \omega g_{v[4]} + \frac{\mu C_p}{P_r}T_y \end{Bmatrix} \tag{10}$$

Ref: Chen, Lee, Liang (2011), JNFM;
Chen, Liang, Lee (2011), JNN.

Transform conservative equations

$$\partial F/\partial x = \partial F/\partial \xi \cdot \partial \xi/\partial \mathbf{x} + \partial F/\partial \eta \cdot \partial \eta/\partial \mathbf{x} + \partial F/\partial \tau \cdot \partial \tau/\partial \mathbf{x} \quad (11)$$

$$\partial G/\partial y = \partial G/\partial \xi \cdot \partial \xi/\partial \mathbf{y} + \partial G/\partial \eta \cdot \partial \eta/\partial \mathbf{y} + \partial G/\partial \tau \cdot \partial \tau/\partial \mathbf{y} \quad (12)$$

$\tilde{Q} = |\mathcal{J}| \cdot Q$

$$\begin{pmatrix} \tilde{F} \\ \tilde{G} \\ \tilde{Q} \end{pmatrix} = |\mathcal{J}| \begin{bmatrix} \xi_x & \xi_y & \xi_\tau \\ \eta_x & \eta_y & \eta_\tau \\ 0 & 0 & 1 \end{bmatrix} \begin{pmatrix} F \\ G \\ Q \end{pmatrix}$$

Transformed conservative equations + Geometric conservation law

$$\frac{\partial \tilde{Q}}{\partial \tau} + \frac{\partial \tilde{F}}{\partial \xi} + \frac{\partial \tilde{G}}{\partial \eta} = 0 \tag{13}$$

$$\frac{\partial |\mathcal{J}|}{\partial \tau} + \frac{\partial (|\mathcal{J}|\xi_t)}{\partial \xi} + \frac{\partial (|\mathcal{J}|\eta_t)}{\partial \eta} = 0 \tag{14}$$

Final set of equations

$$\frac{\partial Q}{\partial \tau} = \frac{1}{|\mathcal{J}|}\left\{ Q\left[\frac{\partial (|\mathcal{J}|\xi_t)}{\partial \xi} + \frac{\partial (|\mathcal{J}|\eta_t)}{\partial \eta}\right] - \left[\frac{\partial \tilde{F}}{\partial \xi} + \frac{\partial \tilde{G}}{\partial \eta}\right]\right\} \tag{15}$$

A five-stage fourth-order Runge-Kutta method for time advancement.

Locating flux and solution points

- $\frac{\partial \tilde{Q}}{\partial \tau} + \frac{\partial \tilde{F}}{\partial \xi} + \frac{\partial \tilde{G}}{\partial \eta} = 0$

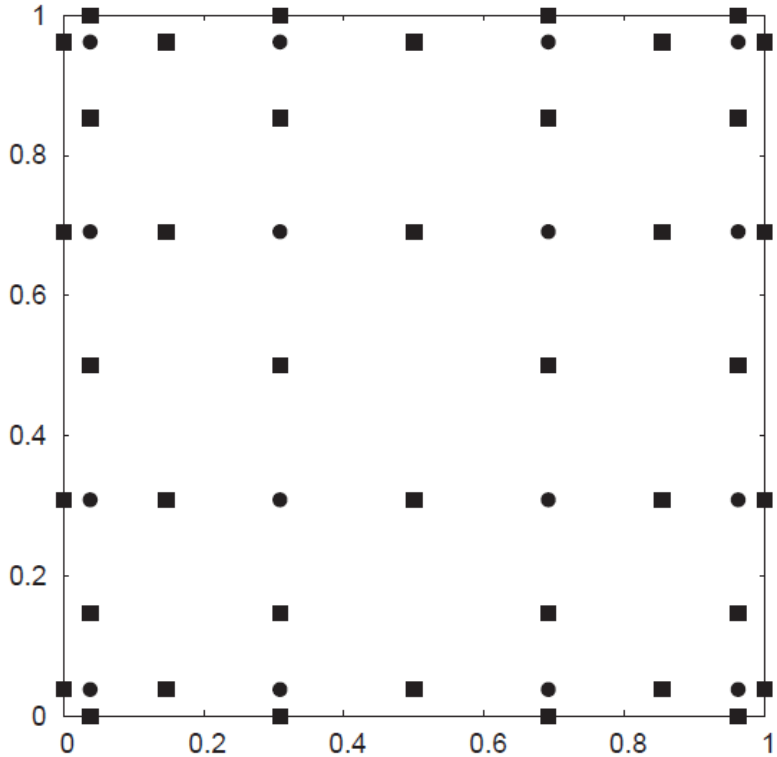

Figure: Solution and flux points for a fourth-order SD scheme

Locating flux and solution points

- $\frac{\partial \tilde{Q}}{\partial \tau} + \frac{\partial \tilde{F}}{\partial \xi} + \frac{\partial \tilde{G}}{\partial \eta} = 0$
- solution points store $\tilde{Q}$, ξ flux points store $\tilde{F}$ and η flux points store $\tilde{G}$.

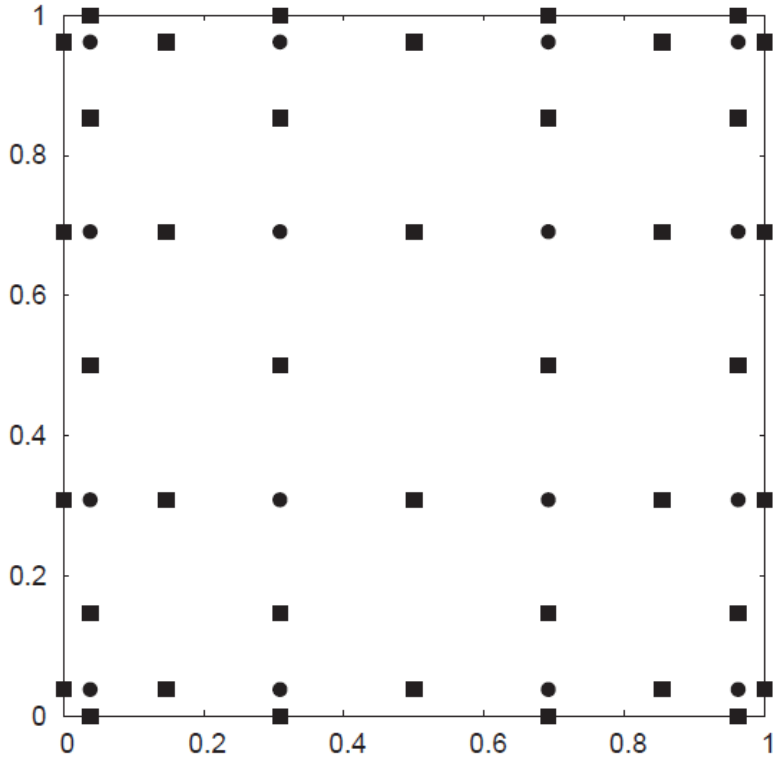

Figure: Solution and flux points for a fourth-order SD scheme

Locating flux and solution points

- $\frac{\partial \tilde{Q}}{\partial \tau} + \frac{\partial \tilde{F}}{\partial \xi} + \frac{\partial \tilde{G}}{\partial \eta} = 0$
- solution points store $\tilde{Q}$, ξ flux points store $\tilde{F}$ and η flux points store $\tilde{G}$.
- 4 solution points in 1D

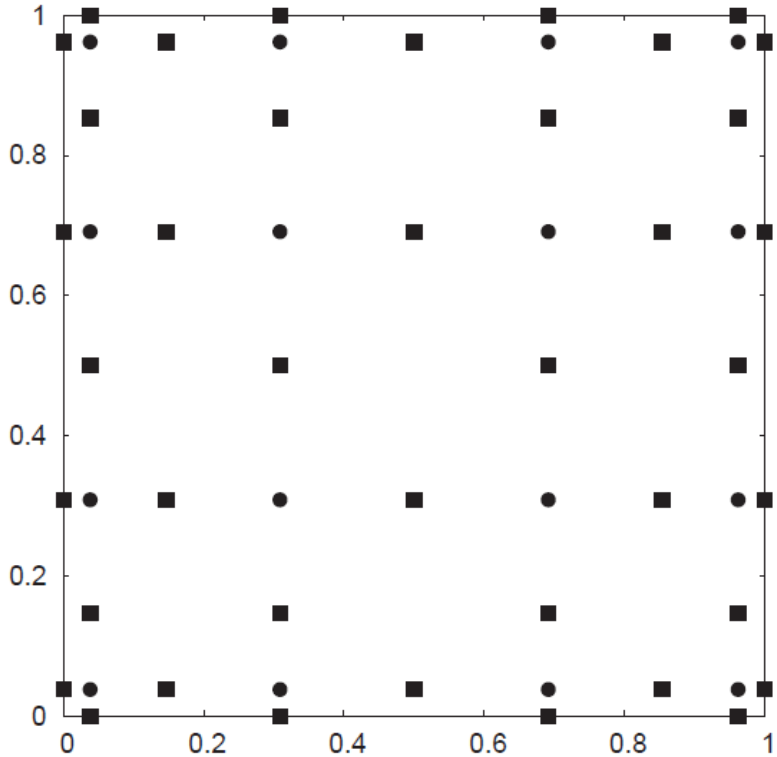

Figure: Solution and flux points for a fourth-order SD scheme

Locating flux and solution points

- $\frac{\partial \tilde{Q}}{\partial \tau} + \frac{\partial \tilde{F}}{\partial \xi} + \frac{\partial \tilde{G}}{\partial \eta} = 0$
- solution points store $\tilde{Q}$, ξ flux points store $\tilde{F}$ and η flux points store $\tilde{G}$.
- 4 solution points in 1D
- 5 flux points in 1D

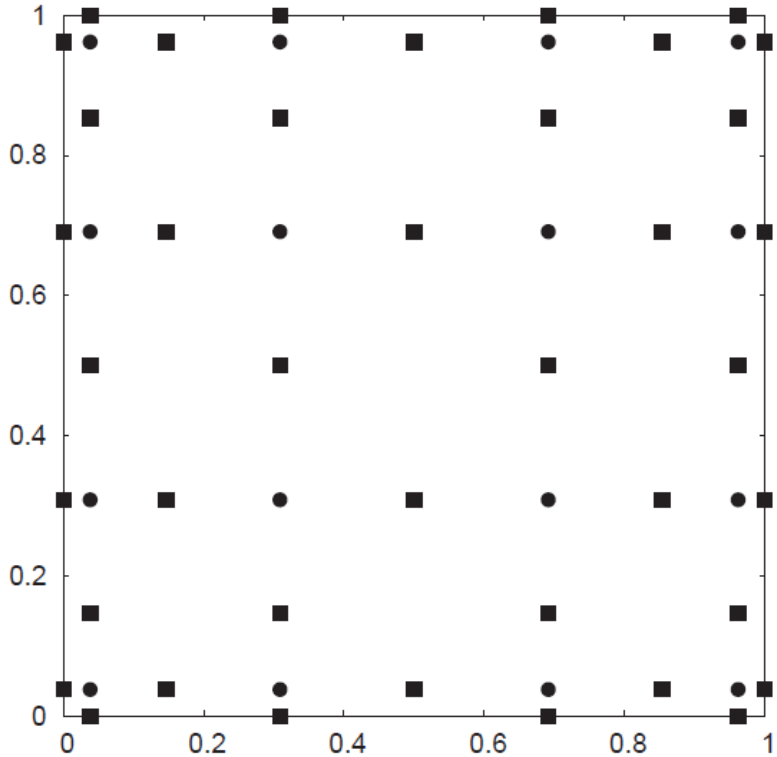

Figure: Solution and flux points for a fourth-order SD scheme

Locating flux and solution points

- $\frac{\partial \tilde{Q}}{\partial \tau} + \frac{\partial \tilde{F}}{\partial \xi} + \frac{\partial \tilde{G}}{\partial \eta} = 0$
- solution points store $\tilde{Q}$, ξ flux points store $\tilde{F}$ and η flux points store $\tilde{G}$.
- 4 solution points in 1D
- 5 flux points in 1D
- The reconstructed field using polynomials is continuous within the cell but discontinuous across the cell interfaces.

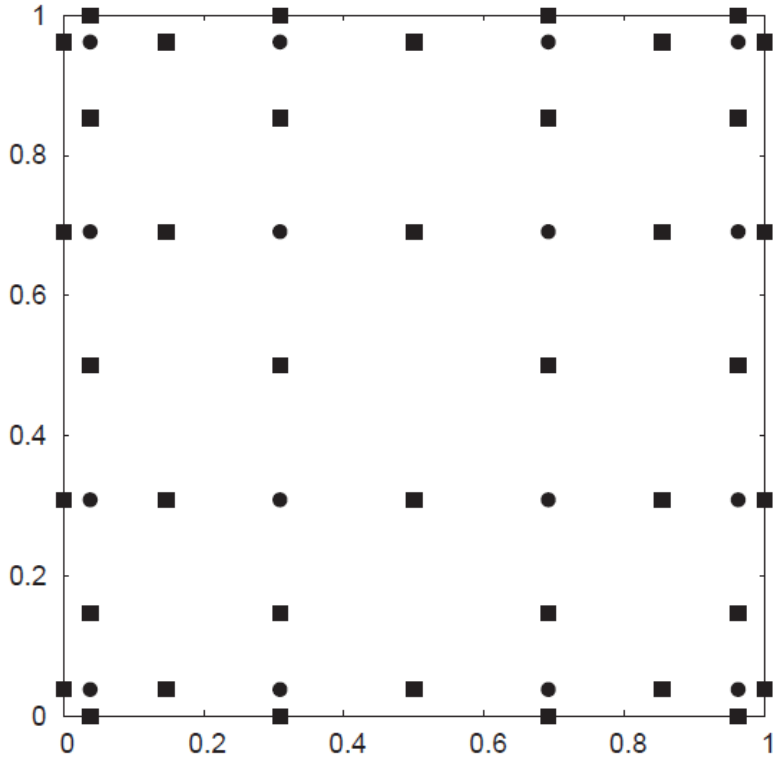

Figure: Solution and flux points for a fourth-order SD scheme

Compute interface fluxes

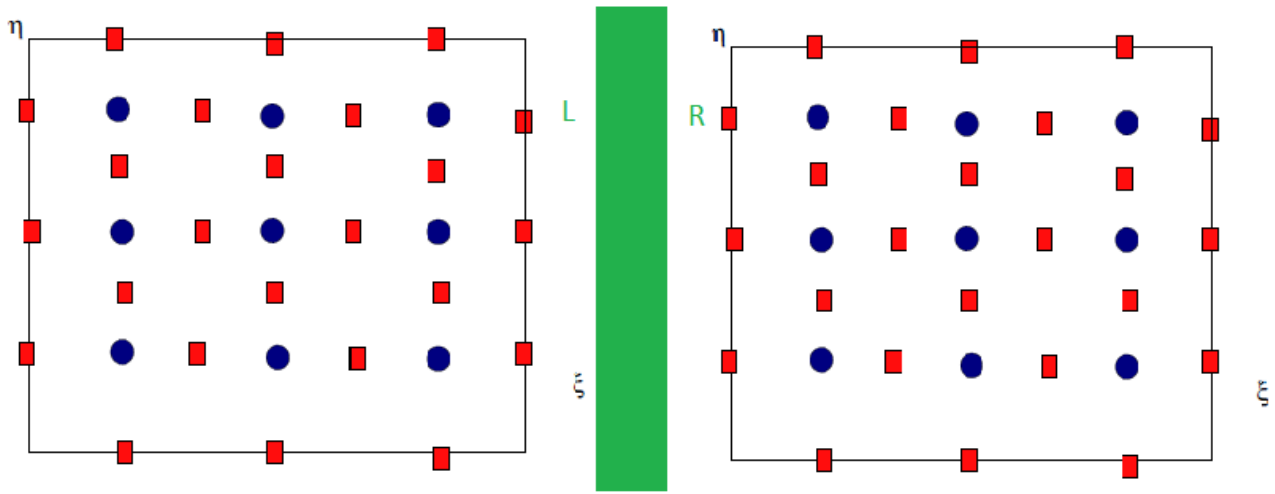

- Eigenvalues of $\partial \mathbf{F}_i / \partial Q$ are $V_n - c$, V_n, and $V_n + c$ for N-S equations.

Compute interface fluxes

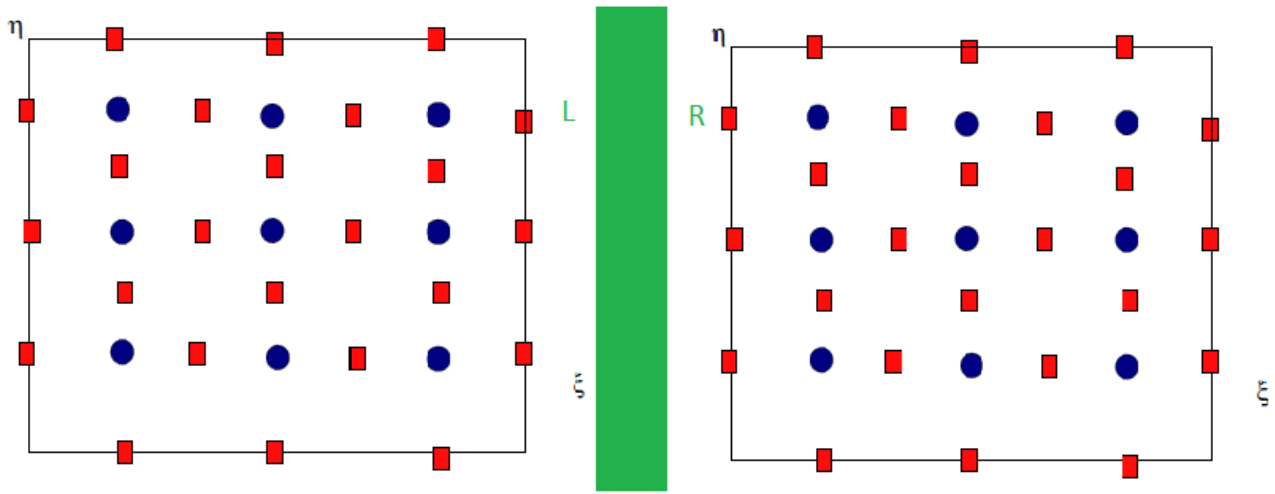

- Eigenvalues of $\partial \mathbf{F}_i / \partial Q$ are $V_n - c$, V_n, and $V_n + c$ for N-S equations.
- Eigenvalues of $\partial \mathbf{F}_i / \partial Q$ are $V_n - c$, V_n, V_n and $V_n + c$ for Micropolar equations.

Compute interface fluxes

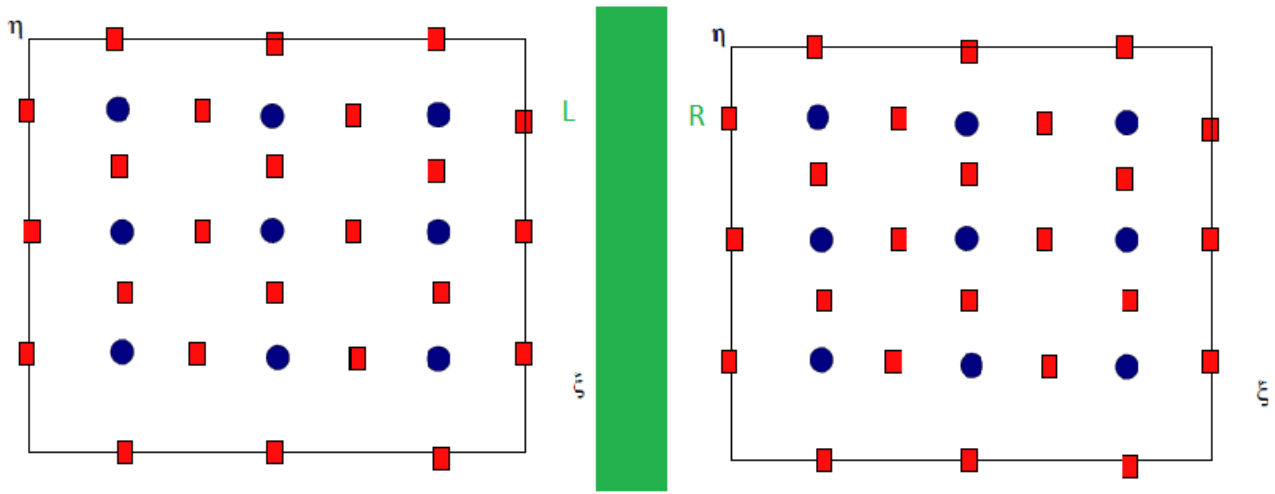

- Eigenvalues of $\partial \mathbf{F}_i / \partial Q$ are $V_n - c$, V_n, and $V_n + c$ for N-S equations.
- Eigenvalues of $\partial \mathbf{F}_i / \partial Q$ are $V_n - c$, V_n, V_n and $V_n + c$ for Micropolar equations.
- Rusanov flux
  $\hat{\mathbf{F}}_{inv} = \frac{1}{2}\left[(\mathbf{F}_i^L + \mathbf{F}_i^R) \cdot \mathbf{n}_f - |V_n + c| \cdot \left(Q^R - Q^L\right)\right]$

Compute interface fluxes

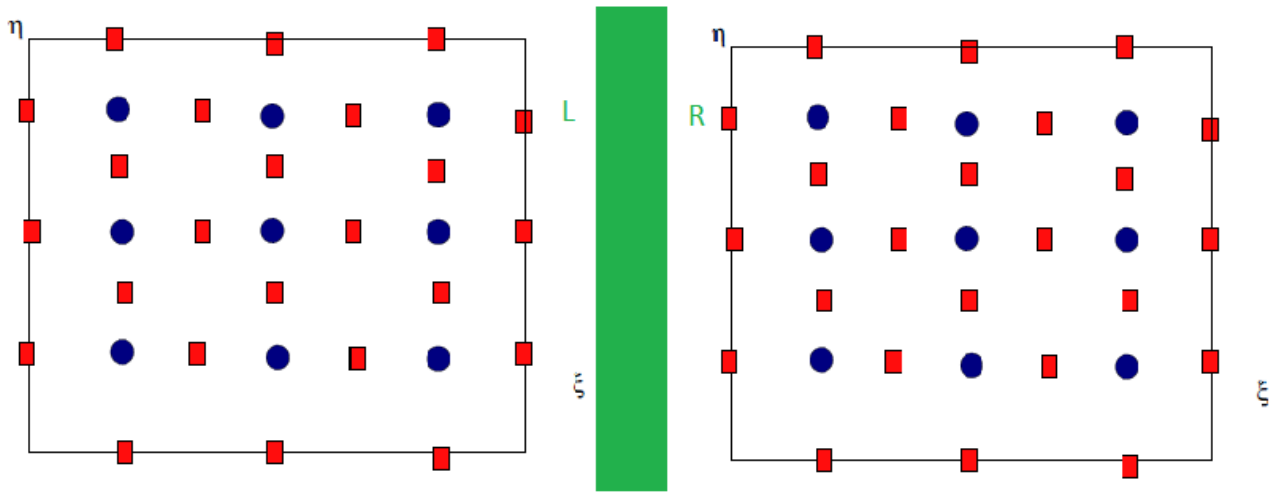

- Eigenvalues of $\partial \mathbf{F}_i / \partial Q$ are $V_n - c$, V_n, and $V_n + c$ for N-S equations.
- Eigenvalues of $\partial \mathbf{F}_i / \partial Q$ are $V_n - c$, V_n, V_n and $V_n + c$ for Micropolar equations.
- Rusanov flux
  $\hat{\mathbf{F}}_{inv} = \frac{1}{2}\left[(\mathbf{F}_i^L + \mathbf{F}_i^R) \cdot \mathbf{n}_f - |V_n + c| \cdot \left(Q^R - Q^L\right)\right]$
- Viscous interface flux – using averaging approach.

Locating solution and flux points

N solution points (One can actually position arbitrarily)

Chebyshev-Gauss points

N+1 flux points

Legendre-Gauss quadrature points plus two end points of 0 and 1.
key difference from Kopriva

$$P_n(\xi) = \frac{2n-1}{n}(2\xi - 1)P_{n-1}(\xi) - \frac{n-1}{n}P_{n-2}(\xi) \qquad (16)$$

where $n = 1, \ldots, N-1$, $P_{-1}(\xi) = 0$ and $P_0(\xi) = 1$
Ref: H. T. Huynh, *AIAA paper*, 2007-4079,
Van den Abeele, Lacor, Wang, *JSC*, 2008,
A. Jameson, *JSC*, 2010.

Verification study for order of accuracy on unstructured grids

No. of cells	DOFs	L2-error	Order	L1-error	Order
3rd order SD					
2	18	8.247E-4	-	7.376E-4	-
8	72	1.501E-4	2.46	1.244E-4	2.57
32	288	1.865E-5	2.99	1.675E-5	2.89
4th order SD					
2	32	2.531E-4	-	1.93E-4	-
8	128	2.19E-5	3.53	1.927E-5	3.55
32	512	1.825E-6	3.585	1.641E-6	3.32

Table: $L2$ and $L1$ errors and orders of accuracy for planar Couette flow

Computational conditions

- $Re = \frac{\rho U_\infty D}{\mu+\kappa} = 185$
- Freestream Mach number $= 0.2$
- j $=$ 1e-6
- $\Gamma = 1e-8$
- Oscillation amplitude $A_y/D = 0.2$,
- Reduced frequency $fD/U_\infty = 0.2145$.

Solution of Navier-Stokes equations

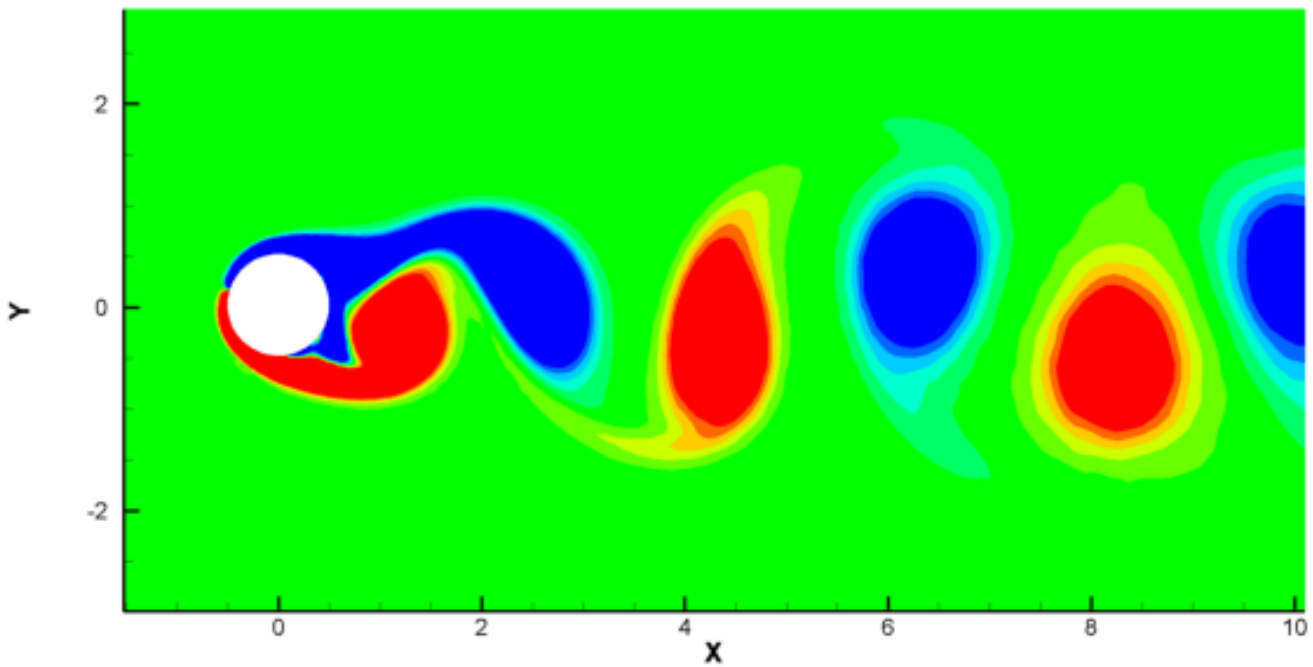

Solution of Micropolar equations ($\mu/\kappa = 0.544$)

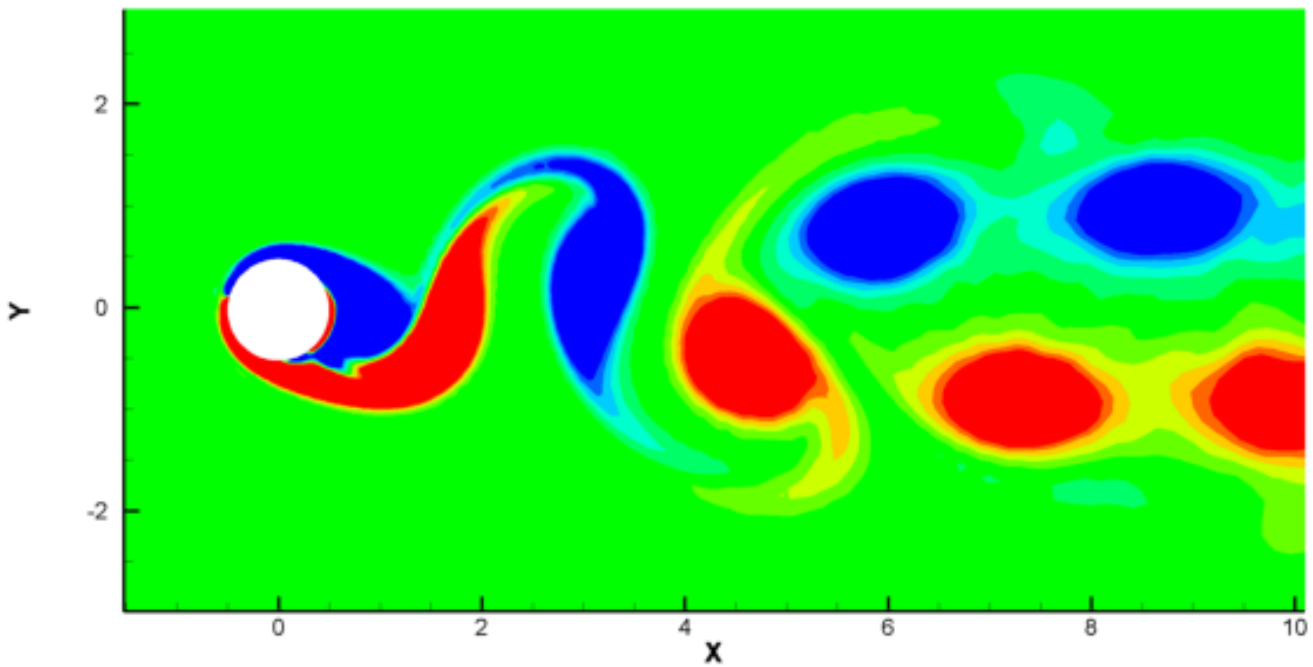

Micropolar effect on lift coefficient

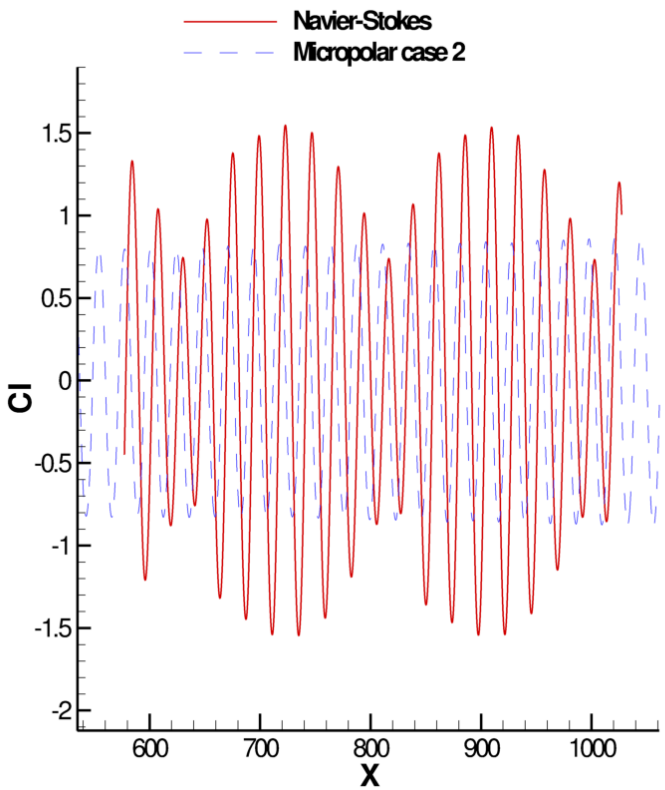

$\mu/\kappa = 0.544$ case v.s. Navier-Stokes

Only one shedding frequency is obtained from Micropolar solution!

Solution of Micropolar equations ($\mu/\kappa = 2.6$)

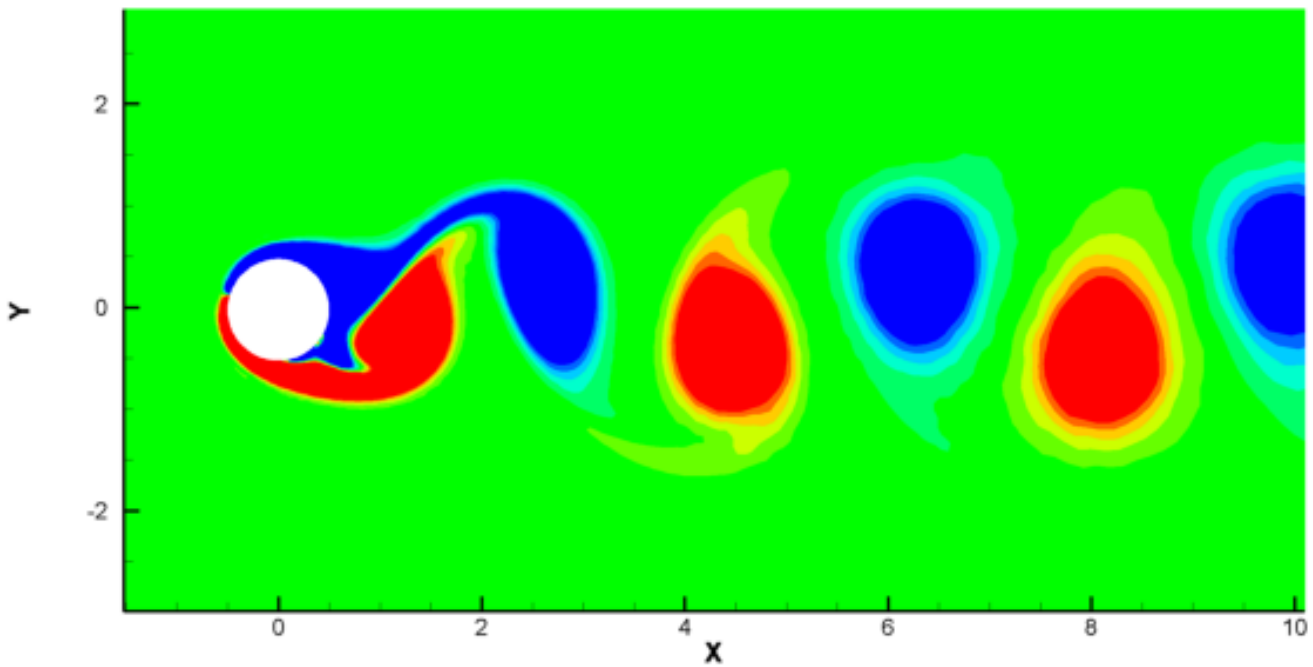

Computational condition for Case I

- $Re = \frac{\rho U_\infty D}{\mu+\kappa} = 500$,
- Mach $= 0.2$,
- $\mu = 8e-4$,
- $\kappa = 1e-3$,
- j = 1e-6,
- $\Gamma = 1e-8$,
- Oscillation amplitude $A_y/D = 0.25$,
- Reduced frequency $fD/U_\infty = 0.1$.

Vorticity contour

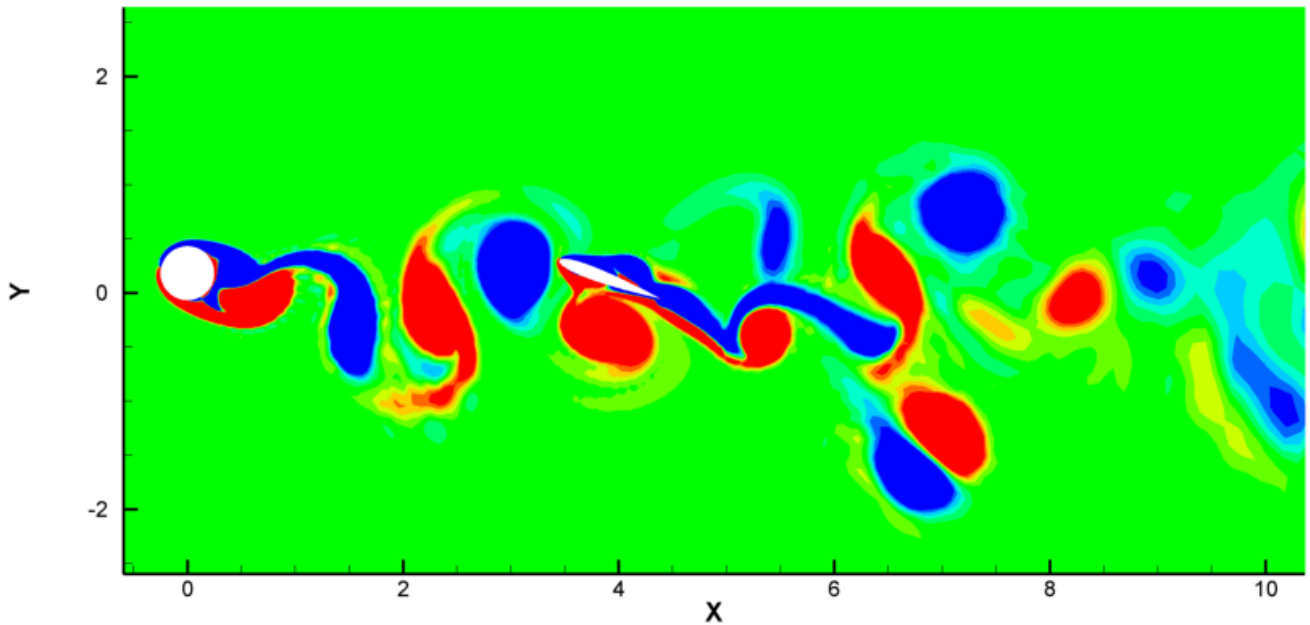

Computational condition for Case II

- $Re = \frac{\rho U_\infty D}{\mu+\kappa} = 500$,
- Mach $= 0.2$,
- $\mu = 8e-4$,
- $\kappa = 1e-3$,
- j = 1e-6,
- $\Gamma = 1e-8$,
- Oscillation amplitude $A_y/D = 0.25$,
- Reduced frequency $fD/U_\infty = 0.5$.

Vorticity contour from Navier-Stokes solution

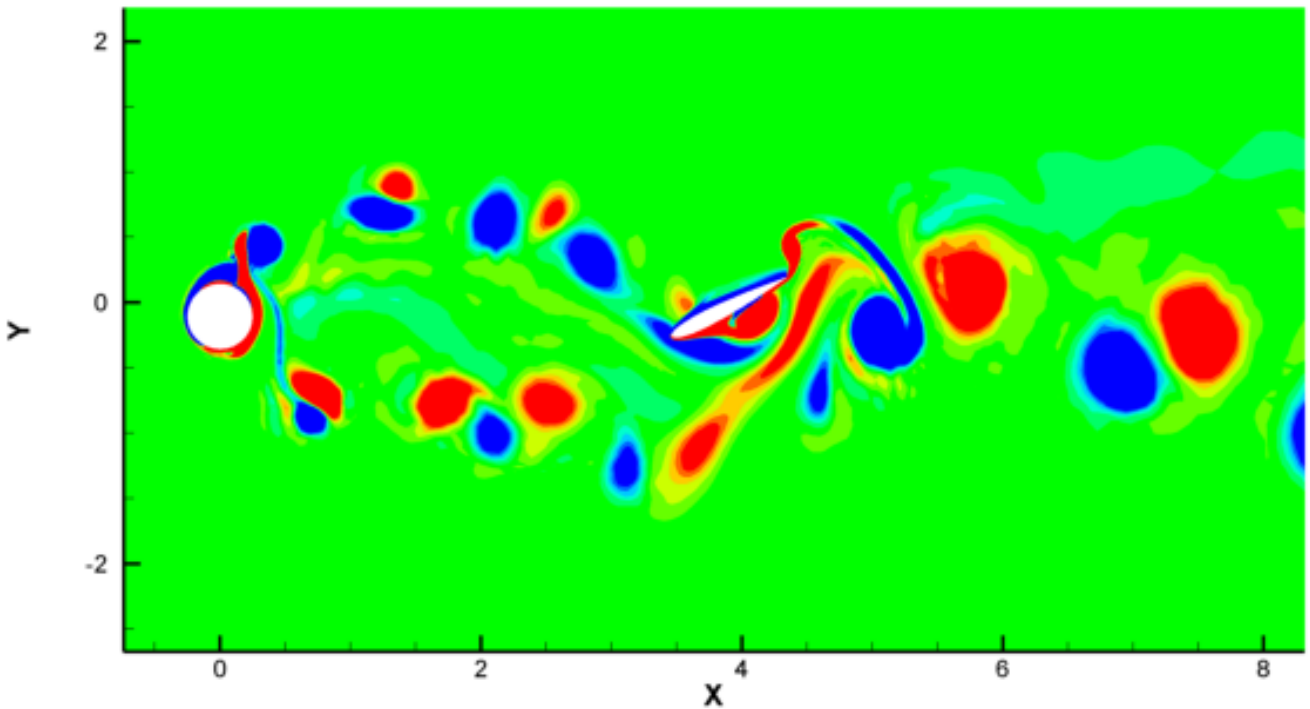

Vorticity contour from Micropolar solution ($\mu/\kappa = 0.54$)

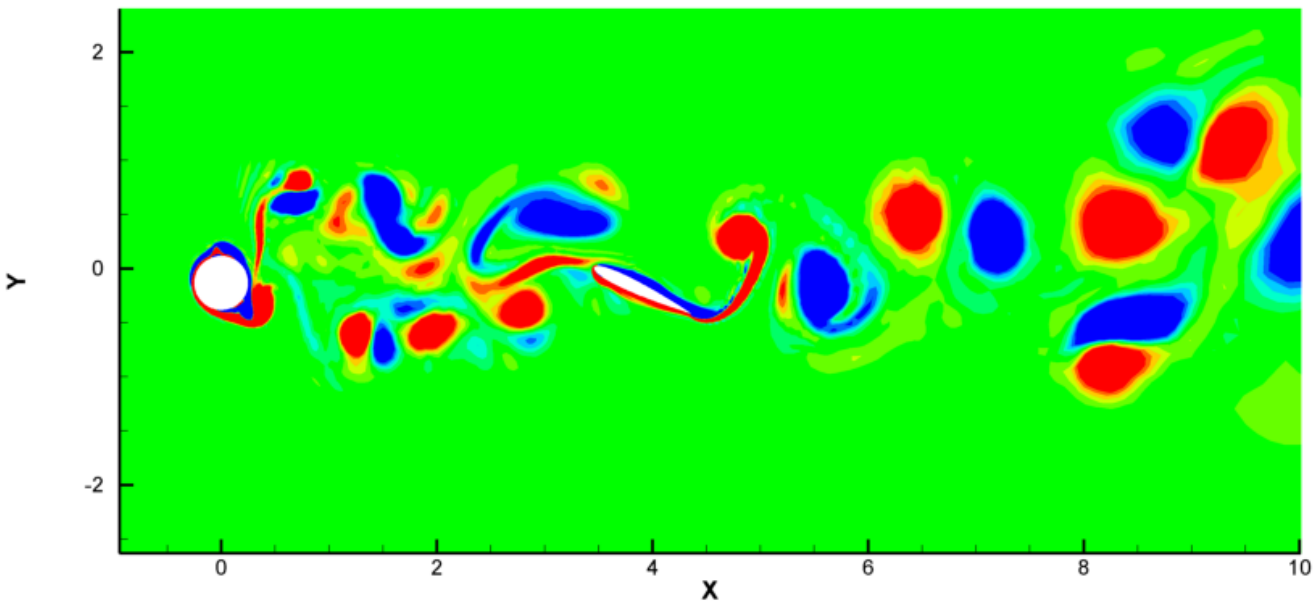

Gyration contour

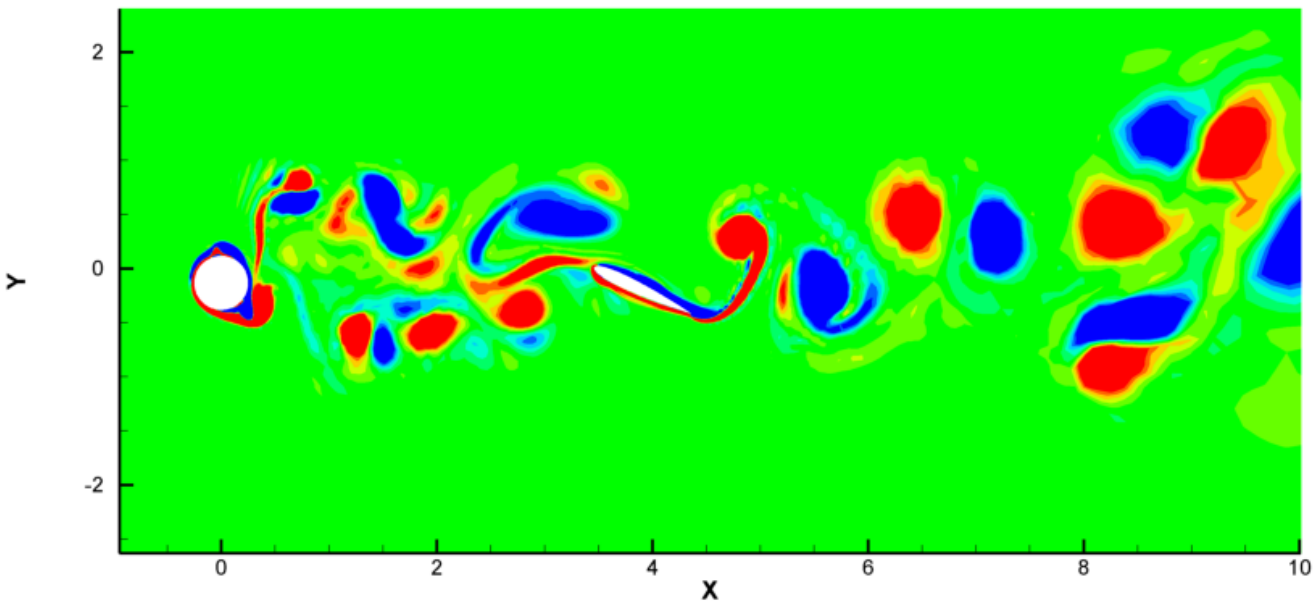

Concluding remarks

- We introduced a new formulation for compressible flow different from Navier-Stokes equations.

Concluding remarks

- We introduced a new formulation for compressible flow different from Navier-Stokes equations.
- SD method is successfully formulated and implemented for unsteady Micropolar flow.

Concluding remarks

- We introduced a new formulation for compressible flow different from Navier-Stokes equations.
- SD method is successfully formulated and implemented for unsteady Micropolar flow.
- Optimal order of accuracy is obtained.

Concluding remarks

- We introduced a new formulation for compressible flow different from Navier-Stokes equations.
- SD method is successfully formulated and implemented for unsteady Micropolar flow.
- Optimal order of accuracy is obtained.
- Extension is successfully made to moving and deformable grids.

Acknowledgement

- George Washington University Faculty Startup Fund

Acknowledgement

- George Washington University Faculty Startup Fund
- GW Graduate Fellowship to James Chen

Acknowledgement

- George Washington University Faculty Startup Fund
- GW Graduate Fellowship to James Chen
- Dr James Chen was co-advised by Prof. James D. Lee and Chunlei Liang

Mesh for a Plunge-Pitch Airfoil

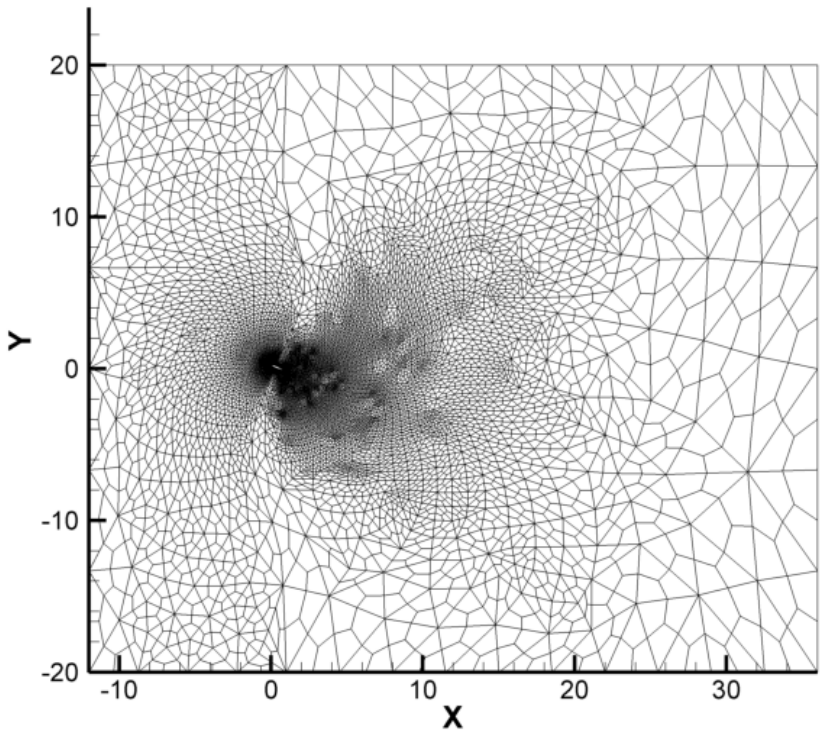

Publications of the SD method

- Liu, Vinokur, Wang, J. Comput. Physics, 2006; *Wave Equations.*
- *Wang, Liu, May, Jameson, J. Scientific Computing, 2007; Euler Equations.*
- *Liang, Jameson, Wang, J. Comput. Physics, 2009; N-S equations.*
- *Chen, Liang, Lee, Computers & Fluids, 2011. Micropolar Equations.*

Multidomain staggered spectral method

Kopriva, J. Comput. Physics, 1998.